Modified Differential Approximation for Radiative Transfer in General Three-Dimensional Media

Michael F. Modest*
Pennsylvania State University, University Park, Pennsylvania

The modified differential approximation first proposed by Olfe for one-dimensional nonscattering media bounded by black walls is extended to the most general case of a three-dimensional, absorbing/emitting and anisotropically scattering medium bounded by nonblack walls. The model reduces to the correct optically-thin and optically-thick limits for all situations. Some one- and two-dimensional solutions are presented, comparing the current method with exact solutions obtained from Monte Carlo calculations, as well as with approximate solutions obtained from the *P*-1 or ordinary differential approximation. Unlike the *P*-1 approximation, the present method is seen to give results of excellent accuracy for all optical conditions, at the price of a very moderate increase in computational effort.

Nomenclature

A = surface area
a_1 = anisotropy factor in scattering phase function
E_n = exponential integral functions
G = incident intensity, Eqs. (9) and (13)
I, I_b = (blackbody) radiative intensity
J = surface radiosity, Eq. (6)
L = length of example cylinder
$\hat{\boldsymbol{n}}$ = unit surface normal
Q = total radiative flux
$q, \boldsymbol{q}$ = radiative flux per unit area, Eqs. (10) and (14)
R = radius of example cylinder
r = radial distance
S = radiative source function, Eq. (2)
s = distance along direction $\hat{s}$
$\hat{s}$ = unit direction vector
β = radiative extinction coefficient
ε = surface emissivity
θ = angle between surface normal and direction vector
τ = optical coordinate, Eq. (5)
Φ = scattering phase function
ψ = azimuthal angle
ω = solid angle
ω_s = single scattering albedo

Subscripts

m = contribution resulting from radiative source within medium
r = radial component
w = contribution resulting from wall emission
z = axial component

Introduction

EXACT calculations of radiative heat flux or its divergence require the solution of very complicated integral equations, in particular if the radiatively participating medium scatters radiation. Large numbers of approximate methods have been proposed, such as 2-flux and 6-flux methods, kernel approximations, *P-N* approximations, etc. (See, for example, standard textbooks such as the ones by Siegel and Howell[1] and Özişik.[2]) All these methods are either tailored to very specific situations (geometry, black walls, radiative equilibrium, and/or nonscattering media, etc.), or they become very cumbersome or inaccurate in more general situations. One particularly popular approximate method is the so-called differential approximation or *P*-1 approximation. This method reduces the calculation of radiative fluxes and temperature fields to the solution of a single linear elliptic partial differential equation, which may be applied to any three-dimensional geometry, with anisotropic scattering as well as boundary reflection (see, for example, Modest and Azad[3]). Unfortunately, the differential approximation is accurate only in optically-thick media, and may become very inaccurate in optically-thin situations, in particular in two- and three-dimensional geometries. This is because, in this method, the directional variation of the intensity is expanded into a Legendre polynomial series truncated after only two terms (P_0 and P_1), i.e., good accuracy can be expected only in situations with near-isotropic intensity fields. To increase the accuracy, a number of improvements have been proposed. Olfe and coworkers[4-8] separated wall emission (which may have strong directional variations) from medium emission (which is isotropic) in what they called the modified differential approximation. While very accurate, their model was limited to nonscattering media of simple geometry bounded by black walls. Modest and coworkers[9-11] combined the *P*-1 approximation with an optically-thin correction term in what they called the improved differential approximation. Even more accurate than Olfe's model, their method was applicable to multidimensional situations with boundary reflection; however, the method was limited to radiative equilibrium and to nonscattering media. Other investigators[12-14] used a higher order differential approximation, the *P*-3 approximation. This method is applicable to general situations but—while more accurate than the ordinary differential approximation—the method is considerably more involved and may still be very inaccurate in optically thin situations.

Recently, Wu et al.[15] demonstrated that—at least for one-dimensional plane-parallel media—Olfe's modified differential approximation may be extended to scattering media with reflecting boundaries. It is the purpose of the present paper to show that the modified differential approximation (or even a higher order modified *P-N* approximation) may be formulated for the general three-dimensional case, with an absorbing/emitting, anisotropically scattering medium bounded

Received May 20, 1988; revision received Sept. 1, 1988; presented as Paper 88-0600 at the AIAA 27th Aerospace Sciences Meeting, Reno, NV, Jan. 9-12, 1989.

*Professor, Department of Mechanical Engineering. Member AIAA.

by nonblack walls. The model reduces to the correct optically-thin and optically thick limits for all situations. Some one- and two-dimensional solutions are presented, comparing the current method with exact solutions obtained from Monte Carlo calculations, as well as with approximate solutions obtained from the P-1 or ordinary differential approximation. Unlike the P-1 approximation, the present method is seen to give results of excellent accuracy for all optical conditions.

Analysis

Consider a three-dimensional enclosure bounded by opaque, diffusely reflecting walls. The equation of radiative transfer for an absorbing, emitting, and scattering medium may be written as[1]

$$\frac{dI}{d\tau}(\boldsymbol{r},\hat{\boldsymbol{s}}) = S(\boldsymbol{r},\hat{\boldsymbol{s}}) - I(\boldsymbol{r},\hat{\boldsymbol{s}}) \tag{1}$$

where I is radiative intensity, τ is optical distance along the ray traveling into a direction $\hat{\boldsymbol{s}}$, as indicated in Fig. 1, and S is the radiative source term given by

$$S(\boldsymbol{r},\hat{\boldsymbol{s}}) = (1-\omega_s)I_b(\boldsymbol{r}) + \frac{\omega_s}{4\pi}\int_{4\pi} I(\boldsymbol{r},\hat{\boldsymbol{s}}')\Phi(\hat{\boldsymbol{s}}\cdot\hat{\boldsymbol{s}}')\,d\omega' \tag{2}$$

Here ω_s is the single scattering albedo, I_b is the black body intensity (Planck function), Φ is the scattering phase function, and ω denotes solid angle. Equation (2) states that the radiative source inside the medium consists of contributions caused by emission and from scattering into direction $\hat{\boldsymbol{s}}$ from all other directions. The preceding equations govern the total radiative intensity for a gray medium, or the spectral intensity if the medium is nongray.

Similar to Olfe,[4] we will now assume that the intensity I at any point consists of two components: one, I_w, that may be traced back to emission from the enclosure wall (but may have been attenuated by absorption and scattering in the medium, and by reflections from the enclosure walls), and the remainder, I_m, which may be traced back to the radiative source term (i.e., radiative intensity released within the medium into a given direction by emission and scattering). Thus we write

$$I(\boldsymbol{r},\hat{\boldsymbol{s}}) = I_w(\boldsymbol{r},\hat{\boldsymbol{s}}) + I_m(\boldsymbol{r},\hat{\boldsymbol{s}}) \tag{3}$$

and let I_w satisfy the equation

$$\frac{dI_w}{d\tau}(\boldsymbol{r},\hat{\boldsymbol{s}}) = -I_w(\boldsymbol{r},\hat{\boldsymbol{s}}) \tag{4}$$

leading to

$$I_w(\boldsymbol{r},\hat{\boldsymbol{s}}) = \frac{J_w}{\pi}(\boldsymbol{r}')e^{-\tau}, \qquad \tau = \int_0^s \beta\,ds' \tag{5}$$

where J_w is radiosity at the wall from where the beam emanates, τ is the optical distance between that point on the wall and the point under consideration (see Fig. 1), and β is the radiative extinction coefficient. Since, for the solution to I_w, no radiative source within the medium is considered, the radiosity in Eq. (5) is the one caused by wall emission only (with attenuation within the medium). The radiosity variation along the enclosure wall may be determined by invoking the definition of the radiosity as the sum of emission plus reflected irradiation, or

$$\begin{aligned} J_w(\boldsymbol{r}) &= \varepsilon\pi I_{bw}(\boldsymbol{r}) + (1-\varepsilon)\int_{|\hat{\boldsymbol{s}}'\cdot\hat{\boldsymbol{n}}|<0} I_w(\boldsymbol{r},\hat{\boldsymbol{s}}')|\hat{\boldsymbol{s}}'\cdot\hat{\boldsymbol{n}}|\,d\omega' \\ &= \varepsilon\pi I_{bw}(\boldsymbol{r}) + (1-\varepsilon)\int_A J_w(\boldsymbol{r}')\frac{\cos\theta\cos\theta'}{\pi s^2}e^{-\tau}\,dA \end{aligned} \tag{6}$$

as indicated in Fig. 2.

Equation (6) is the standard integral equation for the radiosity in an enclosure without a participating medium, except for the attenuation factor $e^{-\tau}$, and may be solved by standard methods such as breaking up the enclosure surface into N small subsurfaces of constant radiosity. Assuming that the attenuation term may be approximated by the value between node centers, this leads to

$$J_i = \varepsilon_i\pi I_{bi} + (1-\varepsilon_i)\sum_{j=1}^{N} J_j e^{-\tau_{ij}}F_{i-j}, \qquad i = 1,N \tag{7}$$

where the F_{i-j} are the configuration factors between the subsurfaces. Evaluation of Eq. (7) is straightforward if the radiative properties of the medium are temperature-independent, or if the temperature field is known; in the case of *radiative equilibrium*, when the temperature field is to be determined, an approximation or iteration may be necessary since, for a temperature-dependent extinction coefficient, the optical distance τ_{ij} depends on the temperature field.

It remains to calculate the contribution from within the medium. Unlike the intensity emanating from the enclosure wall, which may display very irregular behavior (especially in optically thin situations), intensity emanating from inside the medium generally varies very slowly with direction. This is because emission and isotropic scattering result in an isotropic radiation source. Only for highly anisotropic scattering may the radiation source—and, therefore, at least locally, also the intensity—display irregular directional behavior. In the present discussion, we will assume that the medium intensity is adequately represented by the P-1 or differential approximation, i.e., the intensity may be expressed as a series of spherical harmonics, which is truncated after the first harmonic. (Extension to higher order P-N approximations is trivial but tedious.) With this assumption, the medium intensity may be written as[16]

$$I_m \approx \frac{1}{4\pi}(G_m + 3\boldsymbol{q}_m\cdot\hat{\boldsymbol{s}}) \tag{8}$$

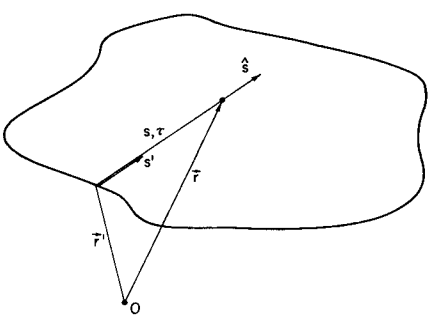

Fig. 1 Radiative intensity within an arbitrary three-dimensional enclosure.

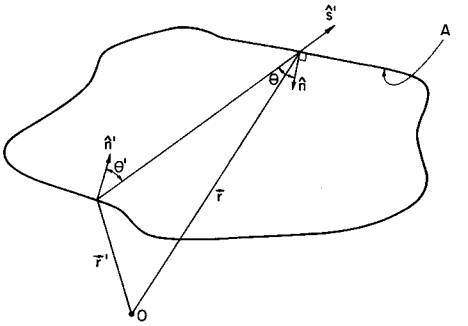

Fig. 2 Coordinates for the determination of wall-related radiosity.

where G_m and $\boldsymbol{q}_m$ are medium related incident intensity and flux, respectively, defined by

$$G_m(\boldsymbol{r}) = \int_{4\pi} I_m(\boldsymbol{r},\hat{\boldsymbol{s}})\, \mathrm{d}\omega \tag{9}$$

$$\boldsymbol{q}_m(\boldsymbol{r}) = \int_{4\pi} I_m(\boldsymbol{r},\hat{\boldsymbol{s}})\, \hat{\boldsymbol{s}}\, \mathrm{d}\omega \tag{10}$$

Such smooth directional behavior can only occur for mildly anisotropic scattering, i.e., expanding the scattering phase function into a series of spherical harmonics, this series must also be truncated after the first harmonic, leading to a *linear-anisotropic* phase function

$$\Phi(\hat{\boldsymbol{s}} \cdot \hat{\boldsymbol{s}}') = 1 + a_1 \hat{\boldsymbol{s}} \cdot \hat{\boldsymbol{s}}' \tag{11}$$

Substituting Eqs. (3), (8), and (11) into Eq. (2) leads then, after carrying out the integration, to

$$S(\boldsymbol{r},\hat{\boldsymbol{s}}) = (1-\omega_s) I_b(\boldsymbol{r}) + \frac{\omega_s}{4\pi} \{G_w(\boldsymbol{r}) + G_m(\boldsymbol{r}) + a_1[\boldsymbol{q}_w(\boldsymbol{r}) + \boldsymbol{q}_m(\boldsymbol{r})] \cdot \hat{\boldsymbol{s}}\} \tag{12}$$

where the wall-related incident intensity and flux are defined similarly to the medium related ones, leading to

$$G_w(\boldsymbol{r}) = \frac{1}{\pi} \int_{4\pi} J_w[\boldsymbol{r}'(\omega)] e^{-\tau}\, \mathrm{d}\omega \tag{13}$$

$$q_w(\boldsymbol{r}) = \frac{1}{\pi} \int_{4\pi} J_w[\boldsymbol{r}'(\omega)] e^{-\tau} \hat{\boldsymbol{s}}\, \mathrm{d}\omega \tag{14}$$

After subtracting Eq. (4), Eq. (1) may now be rewritten as

$$\frac{\mathrm{d}I_m}{\mathrm{d}\tau} = \nabla \cdot (\hat{\boldsymbol{s}} I_m) = (1-\omega_s) I_b + \frac{\omega_s}{4\pi} [G_w + G_m + a_1(\boldsymbol{q}_w + \boldsymbol{q}_m) \cdot \hat{\boldsymbol{s}}] - I_m \tag{15}$$

After integrating over all solid angles, this becomes

$$\nabla \cdot \boldsymbol{q}_m = (1-\omega_s) 4\pi I_b + \omega_s (G_w + G_m) - G_m \tag{16}$$

If Eq. (15) is multiplied by $\hat{\boldsymbol{s}}$ before integration over all directions, this leads to

$$\nabla G_m = a_1 \omega_s (\boldsymbol{q}_w + \boldsymbol{q}_m) - 3\boldsymbol{q}_m \tag{17}$$

Equations (16) and (17) are a complete set of equations for the unknowns G_m and $\boldsymbol{q}_m$. (For higher order P-N approximations, additional equations would need to be generated by multiplying Eq. (15) by successively higher order harmonics before integration.) The necessary boundary conditions for Eqs. (16) and (17) are found by making an energy balance for medium-related radiation at a point on the surface

$$q_m \cdot \hat{\boldsymbol{n}} = \varepsilon \int_{|\hat{\boldsymbol{s}}' \cdot \hat{\boldsymbol{n}}| < 0} I_m(\boldsymbol{r},\hat{\boldsymbol{s}}') \hat{\boldsymbol{s}}' \cdot \hat{\boldsymbol{n}}\, \mathrm{d}\omega' \tag{18}$$

which leads to Marshak's boundary condition for a cold surface[16]

$$2[(2/\varepsilon) - 1] \boldsymbol{q}_m \cdot \hat{\boldsymbol{n}} + G_m = 0 \tag{19}$$

In summary, Eqs. (16) and (17), together with boundary condition (19), comprise a set of equations for the determination of the medium-related incident intensity and flux, with enclosure wall-related incident intensity and flux given by Eqs. (13), (14), and (6). Finally, the total values for incident intensity and flux are given by

$$G = G_w + G_m \tag{20}$$

$$\boldsymbol{q} = \boldsymbol{q}_w + \boldsymbol{q}_m \tag{21}$$

This solution will reduce to the correct solution for the optically-thin limit (when the medium-related contribution vanishes), as well as for the optically-thick limit (where the solution reduces to the unmodified P-1 approximation). For non-scattering or isotropically scattering media, the method requires the additional evaluation of a scalar surface integral for every point in the medium (G_w), whereas for anisotropic scattering G_w as well as a vector surface integral ($\boldsymbol{q}_w$) must be evaluated. If the extinction coefficient is independent of temperature, the G_w (and $\boldsymbol{q}_w$) integrals are purely geometric functions and, thus, may be evaluated once and for all (i.e., they will not enter any iterative process if the temperature field of the medium is to be determined). If the extinction coefficient is temperature dependent, a solution for G_w and $\boldsymbol{q}_w$, based on gross estimates for the temperature field [in order to calculate the optical distances τ_{ij} in Eq. (7)], still will result in the correct optically-thin and -thick limits and, therefore, can be expected to be of reasonable accuracy everywhere in between.

Illustrative Examples

One-Dimensional Slab at Radiative Equilibrium

First we will consider the very simple case of a one-dimensional gray absorbing/emitting and isotropically scattering slab at radiative equilibrium between two isothermal black walls, since this example is a standard by which the accuracy of many models has been assessed. It follows immediately from Eq. (6) that $J_1 = \sigma T_1^4$ and $J_2 = \sigma T_2^4$, where the T_i are the temperatures of the walls. With $q = q_w + q_m = \text{const}$, the solution to Eqs. (16–19) is readily found and the total flux becomes

$$\frac{q_b}{\sigma(T_1^4 - T_2^4)} = \frac{1 + E_3(\tau_0) - (3/2) E_4(\tau_0)}{1 + (3\tau_0/4)} \tag{22}$$

where E_n are exponential integrals and τ_0 is the optical distance between the two plates. Equation (22) is identical to the solution given by Olfe.[4] Comparisons of the results tabulated by Olfe shows that the ordinary differential approximation has a maximum error of $\approx 3.3\%$, as compared to $\approx 1.3\%$ for the modified differential approximation (both at $\tau_0 = 1$). This, however, in no way demonstrates the power of the present method, since this problem is one of the very few in which the ordinary differential approximation actually reduces to the correct optically thin limit.

Two-Dimensional Cold Cylinder With Isotropic Scattering

As a second example, shown in Fig. 3, we will consider a cold gray cylindrical medium of radius R and length L, which absorbs and isotropically scatters radiation, bounded radially and at one of the flat faces by cold black walls. The second face is isothermal at temperature T and has an emissivity of ε. The choice of this example has been prompted by the fact that the author has available to him a *Monte Carlo* code for a two-dimensional cylinder with isotropic scattering and given temperature distributions within the medium and along the walls, making comparison of the present method with "exact" results possible. To make the Monte Carlo calculations numerically efficient and the results more readily displayable, the medium and two of the walls are assumed cold, and the faces and sidewalls are treated as a single node (resulting in total or average flux evaluations).

For this case, it is advantageous to eliminate the flux from Eqs. (16–19), resulting in

$$\frac{1}{\tau_r}\frac{\partial}{\partial\tau_r}\left(\tau_r\frac{\partial G_m}{\partial\tau_r}\right)+\frac{\partial^2 G_m}{\partial\tau_z^2}-3(1-\omega_s)G_m=-3\omega_s G_w \quad (23)$$

subject to the boundary conditions

$$\tau_z=0: \quad \frac{2}{3}\left(\frac{2}{\varepsilon}-1\right)\frac{\partial G_m}{\partial\tau_z}-G_m=0 \quad (24a)$$

$$\tau_z=\tau_L: \quad \frac{2}{3}\frac{\partial G_m}{\partial\tau_z}+G_m=0 \quad (24b)$$

$$\tau_r=\tau_R: \quad \frac{2}{3}\frac{\partial G_m}{\partial\tau_r}+G_m=0 \quad (24c)$$

Here, the τ_r and τ_z are optical coordinates in the radial and axial directions, respectively. The wall-related incident intensity has only a single component, from the face at $\tau_z=0$, leading to (cf. Fig. 3)

$$G_w(r,z)=\frac{1}{\pi}\int_{4\pi}J_w e^{-\tau}\,d\omega$$
$$=2\varepsilon\sigma T^4\left[E_2(\tau_z)-\frac{1}{\pi}\int_0^{\pi}\mu_m(\psi)E_2\left(\frac{\tau_z}{\mu_m}\right)d\psi\right] \quad (25)$$

where $\mu_m(\psi)$ is the cosine of the angle with which the perimenter of the hot disk is seen from a location within the cylinder, i.e.,

$$\mu_m=\frac{z}{\sqrt{z^2+\rho^2}}, \qquad \rho=\sqrt{R^2-r^2\sin^2\psi}-r\cos\psi \quad (26)$$

Once the solution for G_w and G_m has been found, the total flux at $\tau_z=0$ ($z=0$) and $\tau_z=\tau_L$ ($z=L$) is, with $J_1=\varepsilon\sigma T^4$,

$$q_z(r,z=0)=q_{wz}+q_{mz}=\varepsilon\sigma T^4-\frac{\varepsilon}{2(2-\varepsilon)}G_m(r,0) \quad (27)$$

$$q_z(r,z=L)=2\varepsilon\sigma T^4\left[E_3(\tau_L)-\frac{1}{\pi}\int_0^{\pi}\mu_m^2(\psi)E_3\left(\frac{\tau_L}{\mu_m}\right)d\psi\right]$$
$$+\tfrac{1}{2}G_m(r,L) \quad (28)$$

The solution to the modified differential approximation for this cylindrical-geometry problem has been found by finite-differencing the preceding equations, whereas G_w and q_{wz} (the latter only at the bounding surface $z=L$) were evaluated through numerical quadrature.

To assess the accuracy of the present method, and its improvement over the ordinary P-1 approximation, the P-1 method solution has also been calculated by finite differences, whereas an exact solution was obtained with the Monte Carlo code.

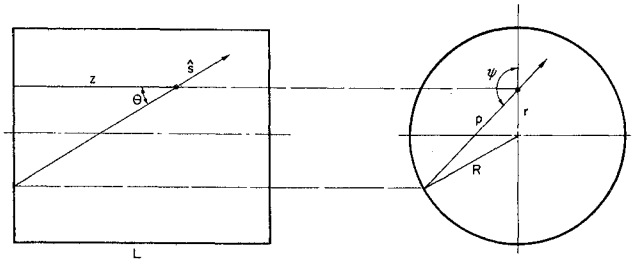

Fig. 3 Coordinate system for two-dimensional cylinder.

The results of this comparison are shown in Figs. 4–7. Figure 4 shows the total normalized flux from the hot surface as function of optical thickness (based on radius) $\tau_R=\beta R$ and scattering albedo ω_s, i.e., the radiative flux integrated over the entire hot surface. In this figure, the hot wall is assumed to be black ($\varepsilon=1$), and the length-to-radius ratio is kept constant at $L/R=2$. It is observed that the modified differential approximation follows the Monte Carlo results very closely for all optical thicknesses and scattering albedos, whereas the ordinary P-1 approximation displays serious errors for optically thin situations. Indeed, it is simple to show that for the ordinary differential approximation, as $\tau_R\to 0$,

$$\left[\frac{q_z(r,z=0)}{\sigma T_w^4}\right]_{\text{ODA}}=\left[\frac{Q_z(z=0)}{\sigma T_w^4\pi R^2}\right]_{\text{ODA}}$$
$$=\frac{\varepsilon}{2-\varepsilon}\left(2-\frac{\varepsilon}{1+(2-\varepsilon)(L/R)}\right) \quad (29)$$

$$\left[\frac{q_z(r,z=L)}{\sigma T_w^4}\right]_{\text{ODA}}=\left[\frac{Q_z(z=0)}{\sigma T_w^4\pi R^2}\right]_{\text{ODA}}$$
$$=\frac{\varepsilon}{1+(2-\varepsilon)(L/R)} \quad (30)$$

while the exact result would be

$$\left[\frac{Q_z(z=0)}{\sigma T_w^4\pi R^2}\right]_{\text{MDA}}=\left[\frac{Q_z(z=0)}{\sigma T_w^4\pi R^2}\right]_{\text{exact}}=\varepsilon \quad (31)$$

$$\left[\frac{Q_z(z=L)}{\sigma T_w^4\pi R^2}\right]_{\text{MDA}}=\left[\frac{Q_z(z=L)}{\sigma T_w^4\pi R^2}\right]_{\text{exact}}$$
$$=\varepsilon\left[1+\frac{1}{2}\left(\frac{L}{R}\right)^2-\frac{L}{R}\sqrt{1+\frac{1}{4}\left(\frac{L}{R}\right)^2}\right] \quad (32)$$

where the latter equation is simply the emissivity multiplied by the configuration factor between parallel disks. Thus, it is seen that the ordinary P-1 approximation gives errors of up to 100% (for large aspect ratios combined with high emissivities), whereas the modified differential approximation always goes to the correct optically thin limit and is, indeed, accurate for all optical thicknesses and all scattering albedos.

Figure 5 shows the identical case for the opposite (cold) face plate, where the P-1 approximation shows the same lack of accuracy, whereas the modified differential approximation

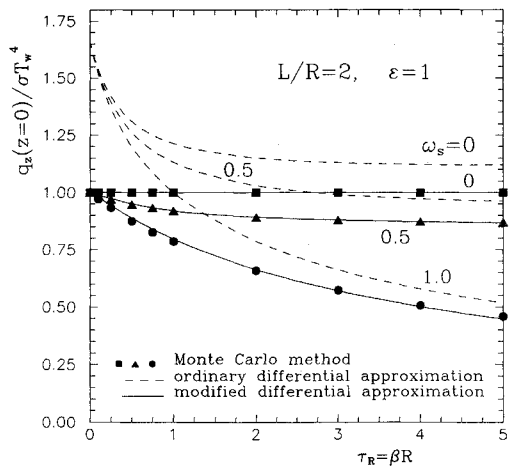

Fig. 4 Normalized flux for cold cylinder enclosed by cold, black liner, one cold face plate and one hot face plate; influence of optical depth and scattering albedo on average flux at hot face plate.

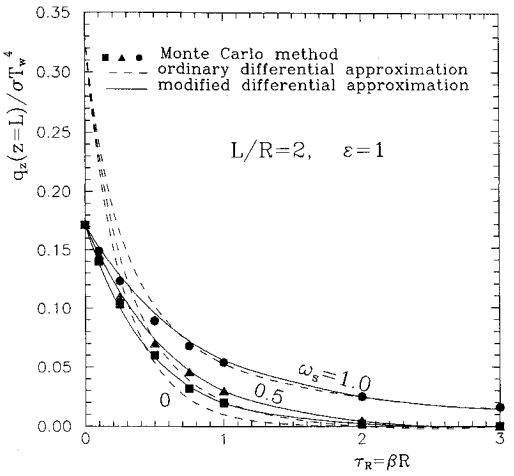

Fig. 5 Normalized flux for cold cylinder enclosed by cold, black liner, one cold face plate and one hot face plate; influence of optical depth and scattering albedo on average flux at cold face plate.

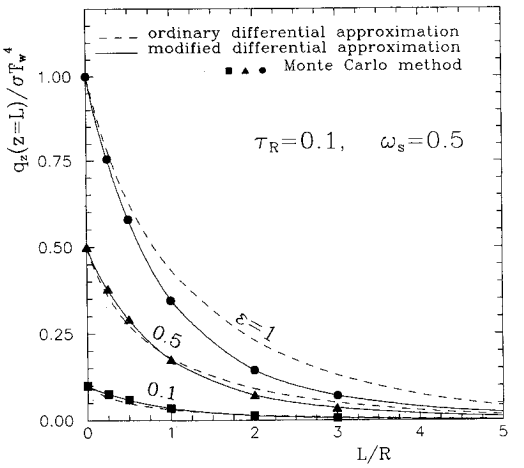

Fig. 7 Normalized flux for cold cylinder enclosed by cold, black liner, one cold face plate and one hot face plate; influence of aspect ratio and surface emissivity on average flux at cold face plate.

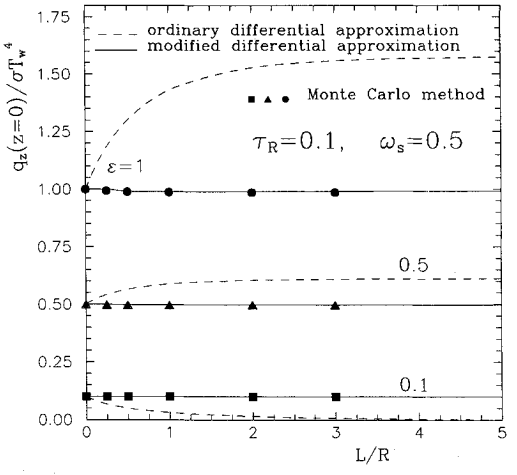

Fig. 6 Normalized flux for cold cylinder enclosed by cold, black liner, one cold face plate and one hot face plate; influence of aspect ratio and surface emissivity on average flux at hot face plate.

again gives good results, with only slight errors for intermediate optical depths, particularly for large scattering albedos.

Figures 6 and 7 show the influence of aspect ratio L/R and of hot-surface emissivity ε on the average flux at the two faces, all for a small optical thickness $\tau_R = 0.1$ (where the P-1 approximation is often inaccurate) and for a scattering albedo of $\omega_s = 0.5$. For $L/R = 0$, one has the optically transparent one-dimensional case and, as expected, even the P-1 approximation gives the correct answer, whereas for growing aspect ratio the predicted flux at the hot face and the error increase rapidly until they reach an asymptotic value (at $L/R \approx 4$). Heat fluxes at the hot face plate predicted by Monte Carlo and by the modified differential approximation remain approximately independent of aspect ratio; with increasing L/R the flux first decreases slightly (never more than 1%) before going back to the original value. The P-1 approximation does fairly well at the cold plate, except for large emissivities, for which the predicted decrease in flux is much too small. Again, the modified differential approximation does very well under all conditions.

Because of the limitations of the available Monte Carlo code, only isotropic scattering was considered in the examples. However, because of its linear-anisotropic description of the intensity field, the P-1 approximation is known to perform equally well for linear-anisotropic scattering.[3] While highly anisotropic scattering cannot be treated by the P-1 or, therefore, the present approximation, it has been well established that highly anisotropic scattering can always be replaced by an equivalent linear-anisotropic phase function for heat transfer calculations.[17] Thus, it is reasonable to expect that the present method will do equally well for any arbitrary scattering situation.

Conclusions

The modified differential approximation first proposed by Olfe for one-dimensional nonscattering media bounded by black walls has been extended to the most general case of a three-dimensional, absorbing/emitting and anisotropically scattering medium bounded by nonblack walls. As with Olfe's original model that was restricted to nonscattering media between black surfaces in simple geometries, the present model reduces to the correct optically-thin and optically-thick limits for all situations. Comparison with exact solutions obtained from Monte Carlo calculations demonstrates that, unlike the standard P-1 approximation, the present method gives results of excellent accuracy for all optical conditions. For nonscattering or isotropically scattering media, the method requires the additional evaluation of a scalar surface integral for every point in the medium, whereas for anisotropic scattering a scalar as well as a vector surface integral ($\boldsymbol{q}_w$) must be evaluated. These integrals are purely geometric functions and do not enter the iterative process for the evaluation of the temperature field (radiative equilibrium, or combined modes heat transfer). Thus, the modified differential approximation, as generalized in this paper, yields high-accuracy radiative heat transfer predictions at the price of a very moderate increase in computational effort over the standard P-1 approximation.

References

[1]Siegel, R. and Howell, J. R., *Thermal Radiation Heat Transfer*, Hemisphere, NY, 1981.

[2]Özişik, M. N., *Radiative Transfer and Interaction With Conduction and Convection*, Wiley, New York, 1973.

[3]Modest, M. F. and Azad, F. H., "The Differential Approximation for Radiative Transfer in an Emitting, Absorbing, and Anisotropically Scattering Medium," *Journal of Quantitative Spectroscopy and Radiative Transfer*, Vol. 23, 1980, pp. 117–120.

[4]Olfe, D. B., "A Modification of the Differential Approximation for Radiative Transfer," *AIAA Journal*, Vol. 5, April 1967, pp. 638–643.

[5]Olfe, D. B., "Application of a Modified Differential Approximation to Radiative Transfer in a Gray Medium Between Concentric

Sphere and Cylinders," *Journal of Quantitative Spectroscopy and Radiative Transfer*, Vol. 8, 1968, pp. 899–907.

[6]Olfe, D. B., "Radiative Equilibrium of a Gray Medium Bounded by Nonisothermal Walls," *Progress in Astronautics and Aeronautics: Thermophysics, Applications to Thermal Design of Spacecraft*, Vol. 23, edited by Jerry T. Bevans, AIAA, New York, 1970, pp. 295–317.

[7]Olfe, D. B., "Radiative Equilibrium of a Gray Medium in a Rectangular Enclosure," *Journal of Quantitative Spectroscopy and Radiative Transfer*, Vol. 13, 1973, pp. 881–895.

[8]Glatt, L. and Olfe, D. B., "Radiative Equilibrium of a Gray Medium in a Rectangular Enclosure," *Journal of Quantitative Spectroscopy and Radiative Transfer*, Vol. 13, 1973, pp. 881–895.

[9]Modest, M. F., "Two-Dimensional Radiative Equilibrium of a Gray Medium in a Plane Layer Bounded by Gray Nonisothermal Walls," *ASME Journal of Heat Transfer*, Vol. C96, 1974, pp. 483–488.

[10]Modest, M. F., "Radiative Equilibrium in a Rectangular Enclosure Bounded by Gray Nonisothermal Walls," *Journal of Quantitative Spectroscopy and Radiative Transfer*, Vol. 15, 1975, pp. 445–461.

[11]Modest, M. F. and Stevens, D., "Two-Dimensional Radiative Equilibrium of a Gray Medium Between Concentric Cylinders," *Journal of Quantitative Spectroscopy and Radiative Transfer*, Vol. 19, 1978, pp. 353–365.

[12]Bayazitoglu, Y. and Higenyi, J., "The High Order Differential Equations of Radiative Transfer: *P*-3 Approximation," *AIAA Journal*, Vol. 17, 1979, pp. 424–431.

[13]Ratzel, A. C. and Howell, J. R., "Two-Dimensional Radiation in Absorbing-Emitting-Scattering Media Using the *P-N* Approximation," *ASME Journal of Heat Transfer*, 1983, pp. 333–340.

[14]Mengüc, M. P. and Viskanta, R., "Radiative Transfer in Axisymmetric, Finite Cylindrical Enclosures," *ASME Journal of Heat Transfer*, Vol. 108, 1986, pp. 271–276.

[15]Wu, C. Y., Sutton, W. H., and Love, T. J., "Successive Improvement of the Modified Differential Approximation in Radiative Heat Transfer," *Journal of Thermophysics and Heat Transfer*, Vol. 1, Oct. 1987, pp. 296–300.

[16]Modest, M. F., "Photon-Gas Formulation of the Differential Approximation in Radiative Transfer," *Letters in Heat and Mass Transfer*, Vol. 3, 1976, pp. 111–116.

[17]Modest, M. F. and Azad, F. H., "The Influence and Treatment of Mie-Anisotropic Scattering in Radiative Heat Transfer," *ASME Journal of Heat Transfer*, Vol. 102, 1980, pp. 92–98.